

GA-A25019

MODULATED CURRENT DRIVE MEASUREMENTS

by

C.C. PETTY, W.A. COX, C.B. FOREST, R.J. JAYAKUMAR,
J. LOHR, T.C. LUCE, M.A. MAKOWSKI, and R. PRATER

APRIL 2005



DISCLAIMER

This report was prepared as an account of work sponsored by an agency of the United States Government. Neither the United States Government nor any agency thereof, nor any of their employees, makes any warranty, express or implied, or assumes any legal liability or responsibility for the accuracy, completeness, or usefulness of any information, apparatus, product, or process disclosed, or represents that its use would not infringe privately owned rights. Reference herein to any specific commercial product, process, or service by trade name, trademark, manufacturer, or otherwise, does not necessarily constitute or imply its endorsement, recommendation, or favoring by the United States Government or any agency thereof. The views and opinions of authors expressed herein do not necessarily state or reflect those of the United States Government or any agency thereof.

MODULATED CURRENT DRIVE MEASUREMENTS

by

C.C. PETTY, W.A. COX,* C.B. FOREST,* R.J. JAYAKUMAR,[†]
J. LOHR, T.C. LUCE, M.A. MAKOWSKI,[†] and R. PRATER

This is a preprint of a paper to be presented at the 16th Topical Conference on Radio Frequency Power in Plasmas, Park City, Utah, April 11–13, 2005 and to be published in the *Proceedings*.

*University of Wisconsin, Madison, Wisconsin.

[†]Lawrence Livermore National Laboratory, Livermore, California.

Work supported by
the U.S. Department of Energy
under DE-FC02-04ER54698, DE-FG03-99ER54541,
and DE-FG02-86ER53224

GENERAL ATOMICS PROJECT 30200
APRIL 2005



Modulated Current Drive Measurements

C.C. Petty*, W.A. Cox[†], C.B. Forest[†], R.J. Jayakumar[‡], J. Lohr*,
T.C. Luce*, M.A. Makowski[‡], and R. Prater*

*General Atomics, P.O. Box 85608, San Diego, California, 92186-5608 USA

[†]University of Wisconsin, Madison, Wisconsin, USA

[‡]Lawrence Livermore National Laboratory, Livermore, California, USA

Abstract. A new measurement approach is presented which directly determines the noninductive current profile from the periodic response of the motional Stark effect (MSE) signals to the slow modulation of the external current drive source. A Fourier transform of the poloidal magnetic flux diffusion equation is used to analyze the MSE data. An example of this measurement technique is shown using modulated electron cyclotron current drive (ECCD) discharges from the DIII-D tokamak.

Several methods are available for determining the noninductive current profile from the measured internal magnetic field structure (e.g. motional Stark effect (MSE) polarimetry [1,2]). In the deductive approach, the noninductive current drive is found from the evolution of the poloidal magnetic flux per radian (ψ) obtained from a time series of magnetic equilibrium reconstructions [3]. In the inductive approach, the measured MSE signals are compared to realistic simulations of the MSE evolution using a coupled transport-equilibrium code that contains a model for the location, width, and magnitude of the current drive source [4]. In this paper, a new modulation approach is presented, where the current drive profile is found directly from the periodic response of the MSE signals to a slow modulation of the external current drive source using the poloidal flux diffusion equation. This yields a local measurement of the noninductive current profile in analogy to measuring the rf power deposition profile from the oscillations in the electron temperature (T_e).

DERIVATION OF MODULATION METHOD

The evolution of ψ is governed by a diffusion equation that is arrived at by combining the flux-surface-average Ampere's, Faraday's and Ohm's laws. In general toroidal geometry, this equation can be written as

$$\frac{\partial \psi}{\partial t} = \frac{\eta}{\mu_0 \rho_b^2 \hat{F}^2} \frac{1}{\rho} \frac{\partial}{\partial \rho} \left(\hat{F} \hat{G} \hat{H} \rho \frac{\partial \psi}{\partial \rho} \right) + \frac{R_0 \eta \hat{H}}{B_{\phi,0}} \langle \vec{J}_{NI} \cdot \vec{B} \rangle, \quad (1)$$

where η is the plasma resistivity, ρ is the normalized toroidal flux coordinate, ρ_b is the effective boundary radius, J_{NI} is the noninductive current density, and $B_{\phi,0}$ is the vacuum field at the center of the plasma boundary (at major radius R_0). The symbol

$\langle \dots \rangle$ denotes a flux surface average. The three dimensionless geometry factors, defined as

$$\hat{F} \equiv \frac{R_0 B_{\phi,0}}{R B_{\phi}} \quad , \quad \hat{G} \equiv \left\langle \frac{R_0^2}{R^2} \rho_b^2 |\bar{\nabla} \rho|^2 \right\rangle \quad , \quad \hat{H} \equiv \frac{\hat{F}}{\langle R_0^2 / R^2 \rangle} \quad , \quad (2)$$

tend towards unity in the infinite aspect ratio, low β , circular equilibrium limit. Considering for the moment the simplified situation where the plasma flux surfaces are fixed in space, the Fourier transform of Eq. (1) yields an ordinary differential equation that relates the modulated current drive source (J_{NI}) to the modulation in the poloidal magnetic flux ($\tilde{\psi}$),

$$\frac{\partial^2 \tilde{\psi}}{\partial \rho^2} + \left[\frac{1}{\rho} + \frac{\partial}{\partial \rho} \ln(\hat{F} \hat{G} \hat{H}) \right] \frac{\partial \tilde{\psi}}{\partial \rho} - \frac{i}{\hat{D}} \tilde{\psi} = -\mu_0 R_0 \rho_b^2 \frac{\hat{F}}{\hat{G}} \left[\langle \tilde{J}_{NI} \rangle + \frac{\tilde{\eta}}{\eta} \langle J_{oh} \rangle \right] \quad , \quad (3)$$

$$\hat{D} = \frac{\eta}{\mu_0 \rho_b^2 \omega} \frac{\hat{G} \hat{H}}{\hat{F}} \quad , \quad (4)$$

where $\tilde{\eta}$ is the modulated resistivity, J_{oh} is the ohmic current density and $\langle J \rangle = \langle \mathbf{J} \cdot \mathbf{B} \rangle / B_{\phi,0}$. Utilizing Eq. (3), the measured modulation in the vertical magnetic field from the MSE signals, $B_z = (1/R) \partial \psi / \partial R$, can be used to experimentally determine the modulated current drive profile. A useful feature of the modulation method is that fiducial comparison discharges are not needed to separate the modulated current drive from the unmodulated noninductive currents since the act of detrending the MSE data to remove the non-oscillating component serves this purpose.

There are several practical complications in using Eq. (3) to measure the current drive profile. First, modulating T_e along with the driven current adds a phantom source to the right hand side of Eq. (3) through the $\tilde{\eta}$ term. This may be unavoidable if one wishes to measure the bootstrap current profile by modulating the pressure profile, but for measurements of an external current source it is preferred to minimize $\tilde{\eta}$ by using a push/pull setup where co- and counter-injecting current sources at the same deposition location alternate during each cycle so that the total heating power remains constant with time. Second, the MSE diagnostic actually measures B_z at fixed (R, z) coordinates rather than at a fixed toroidal flux. Therefore, for moving flux surfaces the contribution of the electric field to the left hand side of Eq. (1) should be written as

$$\frac{\partial \psi}{\partial t} = \frac{\partial \psi}{\partial t} \Big|_{R, z} + \frac{\rho_b^2 B_{\phi,0}}{q} \rho \frac{\partial \rho}{\partial t} \Big|_{R, z} - \rho \frac{\partial \psi}{\partial \rho} \left(\frac{1}{\rho_b} \right) \frac{\partial \rho_b}{\partial t} \approx \frac{\partial \psi}{\partial t} \Big|_{R, z} + R B_z \frac{\partial R_0}{\partial t} \quad , \quad (6)$$

where the final relation is derived assuming concentric elliptical flux surfaces. Oscillations in the \hat{F} , \hat{G} , and \hat{H} factors can give rise to additional phantom source terms in Eq. (3), but these are generally negligible.

To experimentally determine the modulated current drive, the Fourier transform is first taken of the oscillating MSE signals, and the resulting B_z profile is integrated over major radius to convert it to $\tilde{\psi}$. Next $\tilde{\psi}$ is corrected for any periodic movement of the flux surfaces using Eq. (6). The constant of integration for $\tilde{\psi}$ can be taken from the measured oscillation in the surface loop voltage ($V_{\phi,b}$). Alternatively, for off-axis current drive the boundary condition $\tilde{\psi}(\rho=0) = 0$ works well. In the high frequency

limit, which is usually approached since \hat{D} is small except near the plasma boundary, the modulated current drive profile is found from

$$\langle \tilde{J}_{NI} \rangle = \frac{i\omega}{R_0 \eta \hat{H}} \tilde{\psi} - \frac{\tilde{\eta}}{\eta} \langle J_{oh} \rangle = \frac{i\omega}{R_0 \eta \hat{H}} \left(- \int_{R_b}^R R \tilde{B}_z dR + \frac{i}{2\pi\omega} \tilde{V}_{\phi,b} \right) - \frac{\tilde{\eta}}{\eta} \langle J_{oh} \rangle, \quad (7)$$

where R_b is the major radius of the plasma boundary on the low field side. Since the current profile does not have time to change significantly during the modulation period in the high frequency limit, the driven current profile is being determined in effect by the measured back emf. The above equation shows that ψ mirrors the modulated current drive profile (with a 90 deg phase lag); interestingly, the MSE diagnostic actually records a null measurement ($B_z = 0$) at the peak current drive location.

MODULATED ECCD EXAMPLE

The direct measurement of the modulated current drive is demonstrated using the DIII-D discharge shown in Fig. 1, which utilized 3.0 MW of alternating co/counter electron cyclotron current drive (ECCD) at 10 Hz. There was a small residual modulation in T_e because the co and counter heating powers were not matched exactly. This caused a small undesired modulation in η that is neglected in the analysis presented here. The expected MSE response, determined by numerically solving Eq. (3), is shown in Fig. 2 where the amplitude and phase of B_z at the fundamental modulation frequency are plotted as a function of the major radius. The modulated ECCD source had a peak deposition at $\rho = 0.22$, which corresponds to $R = 1.59$ m on the plasma inboard midplane and $R = 1.92$ m on the plasma outboard midplane. The largest value of B_z should occur at locations that have a strong spatial gradient in the ECCD source; it also should be noted that the phase of B_z changes by 180 deg across the major radius of the ECCD peak. The measured MSE response to the modulated ECCD was in qualitative agreement with the numerical simulation, as shown in Fig. 2.

The first direct measurement of the flux-surface-average ECCD profile ($\langle J_{EC} \rangle$) using the modulation method is shown in Fig. 3. Since $\langle J_{NI} \rangle$ found from Eq. (7) actually represents the 0-to-peak amplitude for the sinusoidal component at a single frequency, the magnitude needs to be multiplied by $\pi/2$ to yield the peak-to-peak

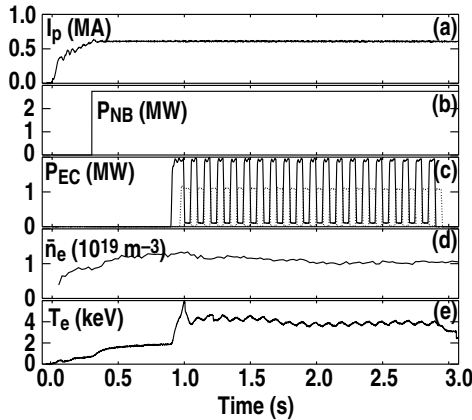


Figure 1. Time history of DIII-D discharge 115425: (a) plasma current, (b) neutral beam power, (c) alternating co-ECCD (solid lines) and counter-ECCD (dotted lines) powers, (d) line average electron density, and (e) central electron temperature.

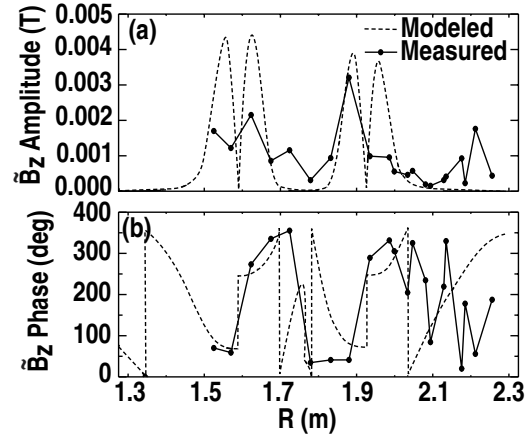


Figure 2. (a) Amplitude and (b) phase (relative to ECCD) of the oscillating vertical magnetic field measured by MSE polarimetry as a function of major radius for DIII-D discharge 115425. Both the modeled (dashed curves) and measured (solid curves and symbols) MSE responses are shown.

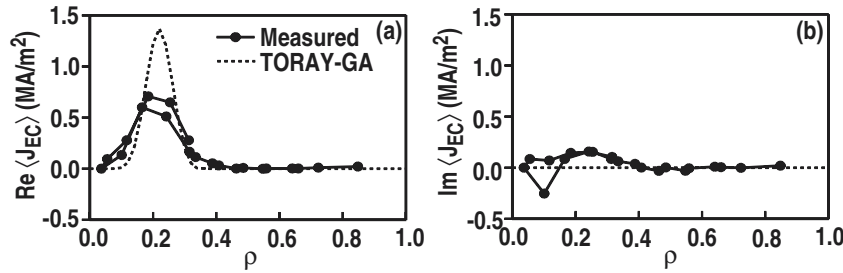


Figure 3. (a) Real and (b) imaginary components of the flux-surface-average ECCD profile as a function of normalized toroidal flux coordinate for DIII-D discharge 115425. Both the experimental (solid curves and symbols) and theoretical (dashed curves) ECCD profiles are plotted.

swing in the driven current density for square wave modulation. The real part of $\langle J_{EC} \rangle$ shown in Fig. 3(a) is the component that is in phase with the modulated ECCD source, whereas the imaginary part of $\langle J_{EC} \rangle$ plotted in Fig. 3(b) is the (90 deg) out of phase component that ideally should be zero. Figure 3(a) shows that localized current drive was measured at the predicted ECCD location, and there was good overlap between the MSE points on the inboard and outboard sides of the axis. Integrating the experimental ECCD profile gives a total driven current (co minus counter) of 0.12 MA, which is in agreement with the predicted ECCD of 0.14 MA from the TORAY-GA ray tracing code [5,6]. However, the TORAY-GA code predicts a more narrow ECCD profile than measured. This could be due to a steering misalignment between the six gyrotrons, or radial diffusion of the current carrying electrons.

CONCLUSIONS

A new method has been developed to directly measure the local current drive profile from internal magnetic measurements such as those from MSE polarimetry. In this approach, the noninductive current profile is determined from the periodic response of the MSE signals to a slow modulation of the current drive source using the poloidal flux diffusion equation. (To measure the bootstrap current profile, the plasma pressure can be slowly modulated.) Corrections to the raw MSE data may be needed to account for oscillations in the plasma flux surfaces and resistivity. The first direct measurement of localized current drive was successfully demonstrated using 10 Hz modulation of ECCD on the DIII-D tokamak.

ACKNOWLEDGMENT

Work supported by the U.S. Department of Energy under DE-FC02-04ER54698, DE-FG03-99ER54541, DE-FG02-86ER53223, W-7405-ENG-48, and the National Undergraduate Fellowships in Plasma Physics and Fusion Energy Sciences.

REFERENCES

1. F.M. Levinton, et al., Phys. Rev. Lett. **63**, 2060 (1989).
2. B.W. Rice, et al., Phys. Rev. Lett. **79**, 2694 (1997).
3. C.B. Forest, et al., Phys. Rev. Lett. **73**, 2444 (1994).
4. C.C. Petty, et al., Nucl. Fusion **41**, 551 (2001).
5. K. Matsuda, IEEE Trans. Plasma Sci. **17**, 6 (1989).
6. Y.R. Lin-Liu, et al., in Controlled Fusion and Plasma Physics (Proc. 26th Euro. Conf., Maastricht, 1999), Vol. 23J (European Physical Society, Geneva, 1999) p. 1245.